

RESEARCH LETTER

10.1002/2014GL061745

Key Points:

- Climate models predict Lorentzian temporal spectra for root zone soil moisture w
- Long-term site measurements deviate from Lorentzian and report shorter w memory
- Precipitation and net radiation impact w spectra and its memory at long scales

Supporting Information:

- Readme
- Texts S1–S3, Figures S1–S5, and Tables S1 and S2

Correspondence to:

T. Nakai,
taro.nakai@gmail.com

Citation:

Nakai, T., G. G. Katul, A. Kotani, Y. Igarashi, T. Ohta, M. Suzuki, and T. Kumagai (2014), Radiative and precipitation controls on root zone soil moisture spectra, *Geophys. Res. Lett.*, 41, 7546–7554, doi:10.1002/2014GL061745.

Received 3 SEP 2014

Accepted 15 OCT 2014

Accepted article online 20 OCT 2014

Published online 5 NOV 2014

Radiative and precipitation controls on root zone soil moisture spectra

Taro Nakai^{1,2}, Gabriel G. Katul^{1,3,4}, Ayumi Kotani⁵, Yasunori Igarashi¹, Takeshi Ohta⁵, Masakazu Suzuki⁶, and Tomo'omi Kumagai¹

¹Hydrospheric Atmospheric Research Center, Nagoya University, Nagoya, Japan, ²International Arctic Research Center, University of Alaska Fairbanks, Fairbanks, Alaska, USA, ³Nicholas School of the Environment, Duke University, Durham, North Carolina, USA, ⁴Department of Civil and Environmental Engineering, Duke University, Durham, North Carolina, USA, ⁵Graduate School of Bioagricultural Sciences, Nagoya University, Nagoya, Japan, ⁶Graduate School of Agricultural and Life Sciences, University of Tokyo, Tokyo, Japan

Abstract Temporal variability in root zone soil moisture content (w) exhibits a Lorentzian spectrum with memory dictated by a damping term when forced with white-noise precipitation. In the context of regional dimming, radiation and precipitation variability are needed to reproduce w trends prompting interest in how the w memory is altered by radiative forcing. A hierarchy of models that sequentially introduce the spectrum of precipitation, net radiation, and the effect of w on evaporative and drainage losses was used to analyze the spectrum of w at subtropical and temperate forested sites. Reproducing the w spectra at long time scales necessitated simultaneous precipitation and net radiation measurements depending on site conditions. The w memory inferred from observed w spectra was 25–38 days, larger than that determined from maximum wet evapotranspiration and field capacity. The w memory can be reasonably inferred from the Lorentzian spectrum when precipitation and evapotranspiration are in phase.

1. Introduction

Fluctuations in root zone soil wetness (w) in time (t) and their associated memory Γ_w (in the time dimension [T]) are drawing significant interest given their controls on a plethora of processes. Γ_w is quantified by the integral time scale computed from the area under the autocorrelation function of w [Katul et al., 2007] but can also be inferred from the decay time scale of the spectrum of w [Delworth and Manabe, 1988]. Γ_w represents how soil “remembers” its wet or dry states long after these conditions have been “forgotten” by the atmosphere [Koster and Suarez, 2001]. It is mainly for this reason that low-frequency variability in w leads to soil moisture memory sufficiently large, so that climatic excursions can “feed-off” on Γ_w [e.g., Delworth and Manabe, 1988; Koster and Suarez, 2001; Seneviratne et al., 2006; Dirmeyer et al., 2013]. Temporal variability in w and Γ_w is also shown to be necessary when forecasting generation of overland flow and links to streamflow in hydrological models [Thompson and Katul, 2012], usable water recharge [Moore et al., 2011], large-scale floods [Milly et al., 2002], mudslides, fire probabilities, or onset of waterborne diseases [Montosi et al., 2012] are impacted by Γ_w . Likewise, ecological models of carbon/water relations [Wu et al., 2012], agriculture-food security [Parent et al., 2006; Lauzon et al., 2004], woody-encroachment issues [Potts et al., 2010], biogeochemical cycling [Guan et al., 2011], and soil microbial processes [Daly et al., 2008] are all tied to variability in $w(t)$ in general and Γ_w in particular. Determining the minimum meteorological variables and soil drivers that control Γ_w is the main objective of this work.

When the budget of w is governed by two hydrological fluxes—a stochastic precipitation series lacking autocorrelation in time (i.e., white noise) and evapotranspirational $ET(t)$ losses that increase linearly with increasing w until a maximum wet surface evapotranspiration ET_{max} is reached, $w(t)$ exhibits a red-noise spectrum originating from water storage within the soil pores at high frequencies [Delworth and Manabe, 1988], and a Γ_w that is inversely proportional to a damping term β [T^{-1}] given as $\Gamma_w = \beta^{-1}$, which is linked to ET_{max} , soil porosity η , and root zone depth R_L via $\beta = ET_{max}/(\eta R_L)$ [Katul et al., 2007]. Under those conditions, the soil moisture spectrum exhibits a well-known Lorentzian form and scales as $((2\pi f)^2 + \beta^2)^{-1}$, where f is frequency (in cycles per unit time). Figure 1 shows the w spectra computed by Delworth and Manabe [1988] (hereafter referred to as DM88) from global circulation models for zonally averaged subtropical and midlatitudinal regions along with the Lorentzian fit to them. It is evident that for small f ($\ll \beta/(2\pi)$), the

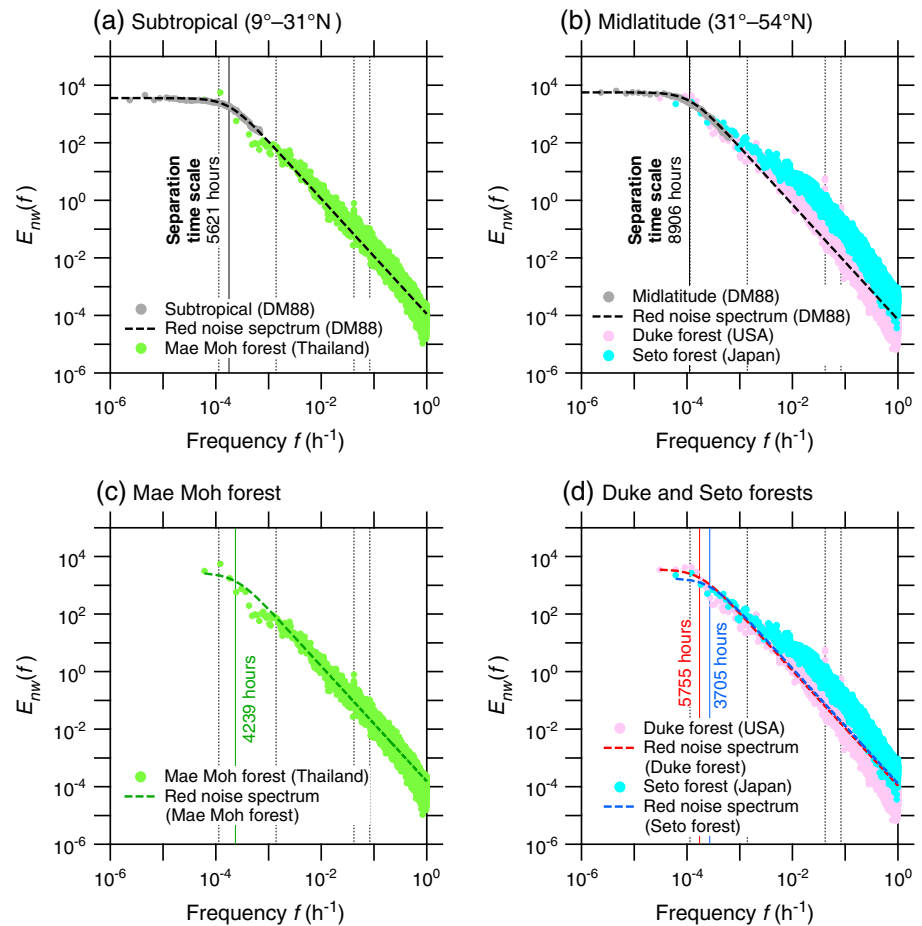


Figure 1. The spectra of normalized soil moisture $E_{nw}(f)$ as a function of frequency f in h^{-1} reported from the original climate model runs of *Delworth and Manabe* [1988] (referred to as DM88) and measured within the root zone at (a) subtropical and (b) midlatitudinal forested sites. Plots of $E_{nw}(f)$ observed in (c) Mae Moh, (d) Duke and Seto forests together with the red-noise spectra fitted to each site. The vertical solid lines represent the *separation time scale* provided by DM88 and obtained in this study, and the vertical dotted lines (right to left) indicate frequencies corresponding to diurnal (12 h), daily (24 h), monthly (720 h), and annual (8760 h) time scales, respectively.

w spectrum in DM88 is flat resembling white noise and for large f ($\gg \beta/(2\pi)$), the w spectra decays as f^{-2} (i.e., red noise). The inferred (constant) β by DM88 appears higher (or Γ_w lower) for subtropical regions when compared to their midlatitudinal counterpart, presumably due to the higher ET_{max} in those regions. This finding received partial support from long-term soil moisture measurements [*Vinnikov et al.*, 1996; *Wu et al.*, 2002]. However, at the ecosystem spatial scale and for time scales ranging from hourly to annual, deviations from a Lorentzian shape are evident in Figure 1 for ecosystems situated within the subtropical and midlatitudinal regions. Also, *Katul et al.* [2007] pointed out that the measured spectrum of precipitation departs from white noise and reveals the $f^{-\alpha}$ (where $\alpha > 0$ is a constant) decay at high frequency when the storm duration is on the order of several hours or less, resulting in the $f^{-2-\alpha}$ decay of soil moisture spectra (i.e., black noise).

More relevant to the objective here is a recent analysis that explored the effects of solar dimming on measured variability in $w(t)$ and suggested that net radiation (R_n) and precipitation patterns are both required, at minimum, to adequately reproduce long-term $w(t)$ trends [*Li et al.*, 2007], a deviation from DM88. Explaining the site-specific deviations from their Lorentzian form shown in Figure 1 and unfolding the role of radiation are the scope of this work. A hierarchy of models that sequentially introduce (i) a realistic spectrum of precipitation beyond its white-noise representation as assumed in DM88, (ii) the spectrum of R_n , and (iii) the dependencies of $ET(t)$ and drainage $D_r(t)$ on $w(t)$ is used to analyze the measured spectra of w and Γ_w from

hour to years at the sites shown in Figure 1. These forested sites are selected because they have comparable maximum leaf area index but markedly different phase relations between (i) $ET(t)$ and $w(t)$, and (ii) precipitation and R_n . It is shown that Γ_w increases with the inclusion of R_n when compared with “precipitation-only” analysis when R_n is characterized by seasonal dynamics not related to precipitation. These findings also suggest that the effect of w dependency of ET and D_r losses on soil moisture spectra appears minor at the sites considered.

2. Theory

2.1. Background and Definitions

Hereafter, $E_x(f)$ and $E_{nx}(f) = E_x(f)/\sigma_x^2$ refer to the actual and normalized one-sided spectra at frequency f of an arbitrary zero-mean stationary stochastic process $x(t)$ with variance $\sigma_x^2 = \int_0^\infty E_x(f)df$. The “memory” of $x(t)/\sigma_x$ can be determined from the autocorrelation function $\rho_x(\tau)$ of $x(t)$ using the definition of the integral time scale Γ_x [Priestley, 1981] given as

$$\Gamma_x = \int_0^{+\infty} \rho_x(\tau) d\tau, \quad (1)$$

where τ is time lag. The $E_{nx}(f)$ is related to $\rho_x(\tau)$ by the Wiener-Khinchin theorem

$$E_{nx}(f) = 2 \int_{-\infty}^{+\infty} \rho_x(\tau) e^{-i2\pi f\tau} d\tau, \quad (2)$$

and since $\rho_x(\tau)$ is an even function, then

$$E_{nx}(0) = 4 \int_0^{+\infty} \rho_x(\tau) d\tau = 4\Gamma_x, \quad (3)$$

resulting in $\Gamma_x = E_{nx}(0)/4$. There lies the problem of determining Γ_x for a finite time series as measured or produced from model runs. To determine $E_{nx}(0)$ requires ad hoc extrapolations of the spectral behavior of $x(t)$ as $f \rightarrow 0$ [Katul et al., 2007]. However, as shown later, these ad hoc extrapolations may be constrained by the energy and hydrological balances.

2.2. The Water Balance in Time and Fourier Domains

The soil-water balance describing stored water $w(t)$ (mm) within the root zone R_L (mm) is given by

$$\frac{dw(t)}{dt} = p(t) - ET(t) - D_r(t), \quad (4)$$

where $p(t)$ is net precipitation (i.e., sum of throughfall and stem flow in mm h^{-1}) at the ground surface assumed to be a constant fraction of rainfall, and $D_r(t)$ is the drainage loss (in mm h^{-1}) at the root zone depth R_L . If the water loss term $L(t) = ET(t) + D_r(t)$ is expressed as $L(t) = L_{\max}w(t)/(\eta R_L)$, then equation (4) can be written in the form used by DM88,

$$\frac{dw(t)}{dt} = -\beta w(t) + p(t), \quad (5)$$

with a damping term $\beta = L_{\max}/(\eta R_L)$ (in h^{-1}), L_{\max} is the maximum loss rate from the root zone water reservoir [Katul et al., 2007]. In this derivation, surface runoff was neglected since occurrence of measured $w \approx \eta R_L$ was not frequent at all sites as shown in Figures S2–S4 in the supporting information.

Upon multiplying equation (5) by $e^{-i2\pi ft}$ and integrating across all t results in

$$i2\pi fW(f) + \beta W(f) = P(f), \quad (6)$$

where $W(f)$ and $P(f)$ are Fourier transforms of $w(t)$ and $p(t)$, respectively. Hence, the Fourier components of $w(t)$ at any f (h^{-1}) are given as

$$W(f) = \frac{P(f)}{i2\pi f + \beta}. \quad (7)$$

The one-sided spectrum of $w(t)$, $E_w(f)$, is given by

$$E_w(f) = 2W(f)W(f)^* = \frac{E_p(f)}{(2\pi f)^2 + \beta^2}, \quad (8)$$

where $W(f)^*$ is the complex conjugate of $W(f)$ and can be determined from equation (7), and $E_p(f) = 2P(f)P(f)^*$ is the one-sided spectrum of $p(t)$. Throughout, the frequency f and not the angular frequency ω (in rad per unit time) is used but the two are related by $\omega = 2\pi f$. If $p(f)$ is random (white noise) as assumed by DM88, $E_p(f) = \sigma_p^2$ is a constant, then equation (5) obeys a first-order Markov process with the soil moisture spectrum represented by a red noise (i.e., f^{-2}) scaling for $f \gg \beta/(2\pi)$ [Delworth and Manabe, 1988; Parlange et al., 1992]. In this case, $\sigma_w^2 = \int_0^\infty E_w(f)df = \sigma_p^2/(4\beta)$, and the normalized soil moisture content spectrum $E_{nw}(f)$ is given by $4\beta/[(2\pi f)^2 + \beta^2]$ resulting in a $\Gamma_w = E_{nw}(0)/4 = 1/\beta$, which is the Lorentzian form presented in Figure 1 (see Text S2 in the supporting information). Moreover, when the primary loss term is dominated by ET, then $L_{\max} = ET_{\max}$ and $\Gamma_w = \eta R_L/ET_{\max}$. All else being the same in terms of η and R_L , increasing ET_{\max} reduces Γ_w as predicted by DM88 in Figure 1 and discussed by the work of Vinnikov et al. [1996] in the context of long-term soil moisture measurements.

2.3. Terminology of Times Scales

The time scale terminology of DM88 is adopted. Specifically, the *decay time scale*, $1/\beta$, is defined as the lag at which $\rho_x(\tau)$ of a first-order Markov process reduces to $1/e$ (e -folding). The *separation time scale*, on the other hand, is a dividing point between the low- and high-frequency limits on the Lorentzian spectrum, which is defined as $2\pi/\beta$. As described in subsections 2.1 and 2.2, the decay time scale is related to $\Gamma_w (= 1/\beta)$. To obtain the decay time scale ($= 1/\beta$), DM88 fitted a red-noise spectrum to the climate-modeled soil moisture spectrum, and the calculated $1/\beta$ is termed *model decay time scale*. On the other hand, the decay time scale defined by $1/\beta = \eta R_L/ET_{\max}$ is termed *evaporative damping time scale*. If these two scales are different, some process other than evaporative damping must play an important role in determining Γ_w .

2.4. Hierarchy of Models

To address the study objective, a series of questions are considered.

1. To what extent does a first-order Markov process capture the variability in w .
2. To what extent should variability in $p(t)$ and in $R_n(t)$ be considered so as to reproduce $E_w(f)$ and Γ_w .
3. If evaporative damping is too short to explain Γ_w , how complex should the $D_r(t)$ dependency on $w(t)$ be when estimating $E_w(f)$ and Γ_w .

To explore these questions, the following hierarchy of models are proposed:

Model 1: The idealized model in equation (8) with the assumption of linear variation of $L(t)$ with $w(t)$ and white noise $p(t)$ is considered as the reference model given its similarity to DM88 and is referred to as "Model 1."

Model 2: The "colored" nature of $p(t)$ is now considered in the framework of Model 1 by including seasonality (i.e., low-frequency correlations) and the temporal structure of storms (high-frequency correlation). To do so, observed $E_p(f)$ is taken into account in equation (8) and this model is referred to as "Model 2."

Model 3: The assumption of linearity in $L(t)$ with respect to $w(t)$ may not be realistic, and other functional forms of $w(t)$ -ET(t) and $w(t)$ - $D_r(t)$ should be independently considered. These considerations were included in a manner so as the time series of $w(t)$ predicted from using equation (4) matches measurements optimally. The $E_w(f)$ from this modeled series is then obtained. Specifically, the following approximations are made to the damping term in equation (4):

$$ET(t) = c\alpha_{PT} \frac{\Delta}{\Delta + \gamma} R_n(t)[s(t)]^a, \quad (9)$$

$$D_r(t) = k_s[s(t)]^b, \quad (10)$$

where c converts energy to mass units (i.e., $W m^{-2}$ to $mm h^{-1}$), α_{PT} is the Priestley-Taylor coefficient [Priestley and Taylor, 1972], $s(t) = w(t)/(R_L\eta) \in [0, 1]$ is a normalized soil moisture content, k_s ($mm h^{-1}$) is a drainage coefficient related to the saturated hydraulic conductivity of the soil, and coefficients a and b describe the effects of soil moisture on ET and D_r , respectively. The case where $a=0$ and $b=0$ is referred to as "Model 3," and this model introduces the effects of R_n variability on $E_w(f)$ and Γ_w without any additional constraints from $s(t)$, while $D_r(t)$ is held constant and not affected by $s(t)$.

Model 4: The final model considers the simultaneous effect of $s(t)$ by taking $b > 1$ for field soils thereby capturing the nonlinearities in the $D_r(t)-w(t)$ relation, and a is set to unity for maximum simplicity and for comparisons with previous models (including DM88) thereby completing the hierarchy. This model is referred to as “Model 4.” It is to be noted that on long time scales, the a and b coefficients need not be constant and can introduce low-frequency variability. By selecting a and b as constants, all the modeled low-frequency variability in w originates from precipitation and net radiation low-frequency variability.

By comparing the $E_w(f)$ and Γ_w from Models 1 to 4 with the observed ones at all three sites, the questions framed here can be readily answered. Note that temporal variability of ET (through R_n effects on potential or Priestley-Taylor ET) and its effects on $E_w(f)$ is only considered in Models 3 and 4.

3. Method

The half-hourly data sets of long-term hydrometeorological measurements collected at Mae Moh forest (Teak plantation in Thailand, March 2006 to February 2012) [Yoshifuji *et al.*, 2006, 2014], Duke forest (Loblolly pine plantation in the USA, January 1998 to December 2005) [Katul *et al.*, 2007], and Seto forest (second-growth deciduous forest in Japan, January 2005 to December 2009) [Matsumoto *et al.*, 2008] were used. The Mae Moe forest is situated in the subtropical region subjected to a tropical monsoon climate, while the Duke and Seto forests are in midlatitude zone characterized by a warm-temperate climate. Further details are provided in the supporting information (Table S1 and Figure S1). MATLAB R2014a version 8 (MathWorks, USA) was used to estimate measured spectra by the Welch averaged modified periodogram method [Welch, 1967] using a Hamming window of length $n/4$, where n is the length of the multiyear records. This window length was an acceptable compromise between the need to resolve low-frequency variations (seasonal to interannual) and the necessity for smoothness to delineate patterns and power laws. The coefficients α_{PT} , k_s , a , and b in equations (9) and (10) for Models 3 and 4 were determined by the combination of a nonlinear least squares method and iterations so that the differences between modeled and observed ET(t) and $w(t)$ are smallest. Details and values of the coefficients are provided in Text S1 and Table S2 in the supporting information.

4. Results

From comparisons between measured and modeled $E_w(f)$, the following can be noted (at increasing time scales).

Diurnal to Daily Time Scales. Measured $E_{nw}(f)$ approximately scales as $f^{-2-\alpha}$ for f varying from 1 h to 1 day (storm duration) as in Figure 2. Steepening beyond Lorentzian (i.e., $\sim f^{-2.6}$) in $E_{nw}(f)$ across all three sites can be reasonably explained by a power law scaling in the measured precipitation spectrum $E_{np}(f) \sim f^\alpha$ ($\alpha \in 0.79-0.85$) (as predicted by Model 2, see Figure 3) at the storm duration scales. Convective and frontal storms spectra for subhourly to daily often exhibit approximate power law scaling with $\alpha = 0.5-1.0$ [Fraedrich and Larnder, 1993; Molini *et al.*, 2009] consistent with measured α at all three sites here. A mixture of such storms exists at all sites resulting in $E_{np}(f) \sim f^{-0.8}$ and explains the onset of $f^{-2-0.8}$ scaling in $E_{nw}(f)$ of Figure 2. Computed Priestley-Taylor ET spectra (primarily driven by R_n) $E_{nRn}(f)$ at all three sites shown in Figure 2 exhibit multiple energetic modes at the hourly-to-daily time scales (and Models 3–4 include all of them). However, those R_n modes appear to have minor effects on measured $E_{nw}(f)$ for the hourly to daily time scales (Figure 2), at least when compared to rainfall (presumably due to R_L being on the order of tens of cm). An interesting outcome from the fact that the $E_{nw}(f)$ decays faster than f^{-2} at all three sites, and that R_n variability has minor effects on $E_{nw}(f)$ is that little fractional variance is lost if sub-daily variability in w is neglected all together. This simplification was adopted in previous eco-hydrological models forced by daily rainfall statistics [Kumagai *et al.*, 2004; Kumagai and Porporato, 2012; Daly *et al.*, 2008; Porporato *et al.*, 2004; Miller *et al.*, 2007] without justification.

Daily to Monthly Time Scales. For time scales varying from daily to about 3 months (and longer at the two midlatitudinal sites), $E_{np}(f)$ scales as f^0 (approximately white noise) consistent with DM88. Measured $E_{nRn}(f)$ is also approximately white noise for the Duke and Mae Moh forests for this range of time scales but not at the Seto forest, where monthly variations in R_n exhibit some scaling. At the Duke and Mae Moh forests, $E_{nw}(f)$ shown in Figure 2 reasonably scales as f^{-2} consistent with DM88 with no seasonal radiation patterns. However, the lower frequency end at which the f^{-2} scaling in $E_{nw}(f)$ ceases to exist at the Seto forest is commensurate with time scales smaller than monthly.

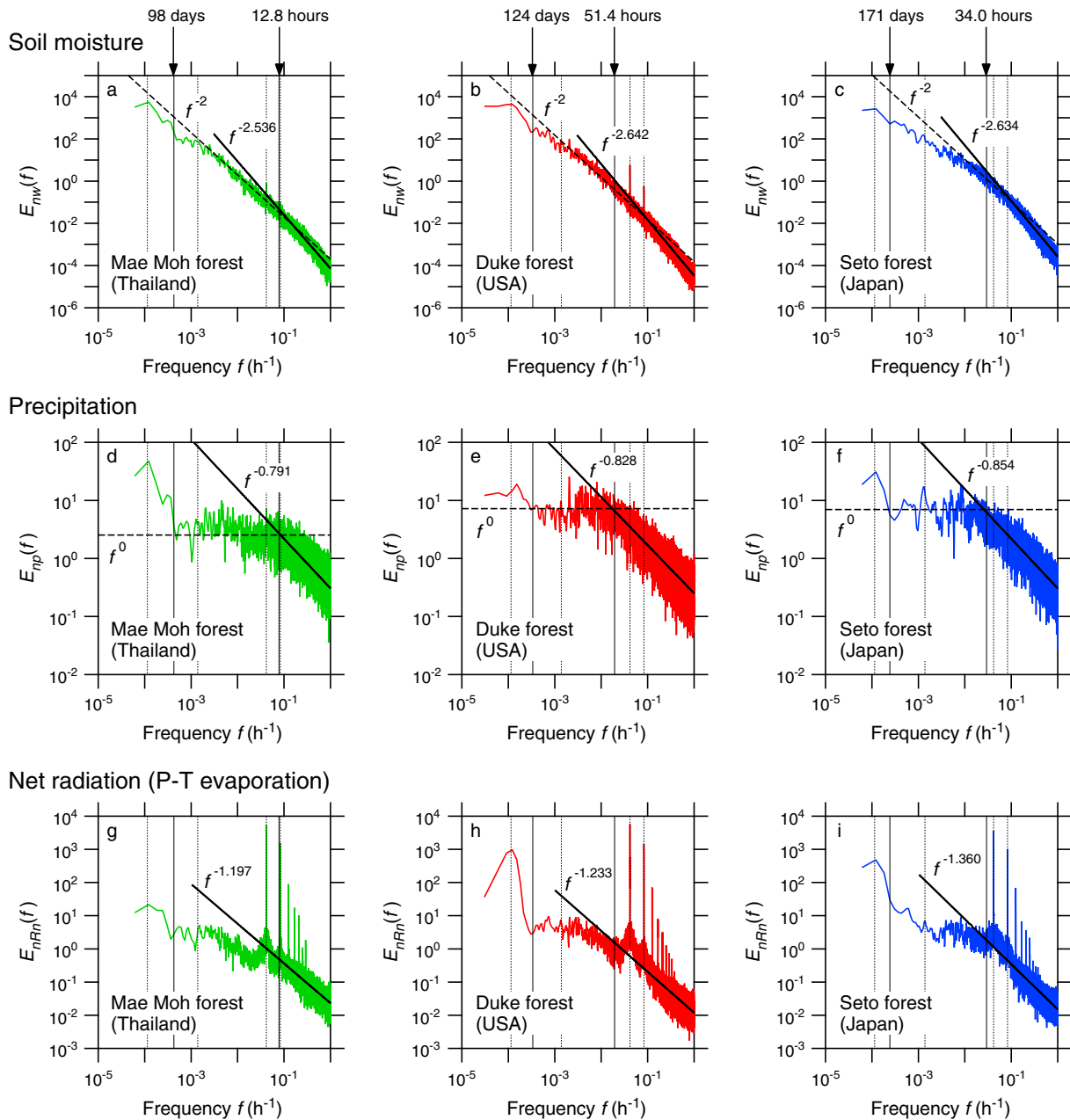


Figure 2. The spectra of (a–c) normalized soil moisture $E_{nw}(f)$ as a function of frequency f measured within the root zone at the three sites along with the (d–f) normalized spectra of precipitation $E_{np}(f)$ and (g–i) evapotranspiration $E_{nRn}(f)$ estimated by the Priestley-Taylor (P-T) formulation (i.e., driven by net radiation) are shown. The green lines (Figures 2a, 2d, and 2g), red lines (Figures 2b, 2e, and 2h), and blue lines (Figures 2c, 2f, and 2i) show the data of Mae Moh, Duke, and Seto forests, respectively. The power laws shown are determined from regression analysis for f^{-1} ranging from 1 to 24 h. Note that when $E_{np} \sim f^{-\alpha}$, $E_{nw} \sim f^{-\alpha-2}$ for this range of f . For reference, the f^{-2} scaling is shown in the $E_{nw}(f)$ (Figures 2a–2c). The vertical solid lines represent the time scale at which a white-noise spectrum (f^0) in $E_{np}(f)$ of each site ceased to exist, and the vertical dotted lines (right to left) indicate frequencies corresponding to diurnal (12 h), daily (24 h), monthly (720 h), and annual (8760 h) time scales, respectively.

Monthly to Annual Time Scales. The results of Models 2 to 4 shown in Figure 3 suggest that variability in $E_w(f)$ beyond seasonal time scales cannot be explained by precipitation spectra alone (Model 2) except for the Seto forest, and seasonality in R_n (tied to the ET spectra through the Priestley-Taylor equation) becomes necessary (Model 3) as previously noted by Li *et al.* [2007]. Comparing Models 3 and 4 also suggests that the dependencies of $ET(t)$ and $D_r(t)$ on $w(t)$ are not as critical to recovering measured $E_w(f)$ at those long time scales, but the inclusion of net radiation is necessary at such long time scales.

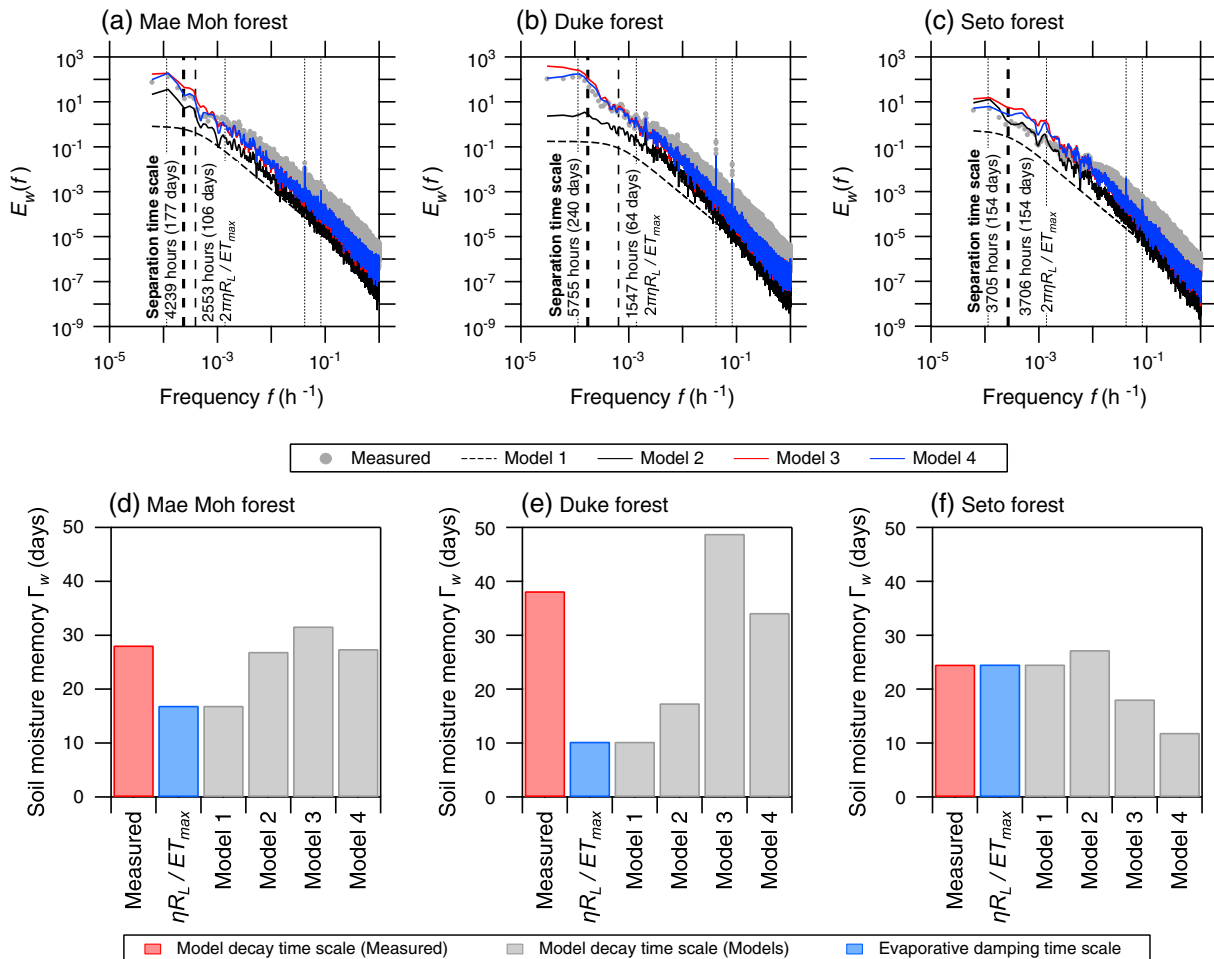


Figure 3. The spectra of soil moisture $E_w(f)$ as a function of frequency f measured within the root zone at (a) Mae Moh, (b) Duke, and (c) Seto forests along with the estimated $E_w(f)$ by the Models 1–4 are shown. The thick and thin vertical dashed lines represent the separation time scales determined by the model time scale for the measured $E_w(f)$ and that from the evaporative damping time scale (i.e., $2\pi\eta R_L/ET_{max}$), respectively, and the vertical dotted lines (right to left) indicate frequencies corresponding to diurnal (12 h), daily (24 h), monthly (720 h), and annual (8760 h) time scales, respectively. Figures 3d–3f show the soil moisture memory Γ_w at (d) Mae Moh, (e) Duke, and (f) Seto forests determined as the model decay time scale of the measured and modeled $E_w(f)$ shown in Figures 3a–3c, together with the evaporative damping time scale $\eta R_L/ET_{max}$.

5. Discussion and Conclusion

Site-specific characteristics appear most evident in $E_w(f)$ for monthly to interannual time scales. In the Seto forest, $E_w(f)$ was reasonably represented by Model 2 (precipitation only). Both ET (loss) and rainfall (gain) exhibit similar (or in-phase) seasonal variation, whereas seasonality in measured $w(t)$ was not evident partly due to compensating effects of p and ET (see Figure S4 in the supporting information). As a result, the maximum of $E_w(f)$ in Seto was 1 order of magnitude smaller than the other two forests, and temporal variability in $w(t)$ was mainly accounted for by variability in p . The $E_w(f)$ at the lowest-frequency end in Mae Moh forest was mainly explained by the addition of precipitation forcing. The effect of adding variability in R_n enhanced the agreement between measured and modeled $E_w(f)$, though not appreciably. Seasonal variations in $w(t)$ were related to the onset and offset of the rainy season in this forest, and seasonality in ET appeared minor (see Figure S2 in the supporting information). In Duke forest, Model 2 was insufficient to explain $E_w(f)$ at longer time scales and seasonality in R_n proved to be necessary. In this forest, measured soil moisture and ET were out of phase, indicating that seasonal variations in $w(t)$ was mainly explained by ET (induced by R_n), while variations in $p(t)$ were nearly random (approximated by a white-noise (f^0) spectrum) (see Figure S3 in the supporting information). Figures 3d–3f show Γ_w for all models and measurements determined by the model decay time scale, together with the evaporative damping scale $\eta R_L/ET_{max}$. These site-specific estimates were all smaller than reported in DM88 (see Figure 1). The model decay time scale of the measured

$E_w(f)$ was largest in Duke forest, whereas the evaporative damping time scale $\eta R_L/ET_{\max}$ was largest in the Seto forest. In the Seto forest, the model decay time scale of the measured $E_w(f)$ was nearly the same as $\eta R_L/ET_{\max}$ and Γ_w by Model 1 and 2, indicating that evaporative damping alone is sufficient to recover the soil moisture memory in this forest (as assumed in DM88). However, Γ_w by Models 3 and 4 underestimated the observed one in Seto despite the fact that only these two models can recover the variability in ET as shown in supporting information (Figure S5). In this site, the $E_w(f)$ was somewhat overestimated around $f \sim 10^{-3}$ (h^{-1}) by adding the effect of R_n , which resulted in the underestimation of Γ_w . Comparing Γ_w inferred from Model 2 with the one inferred from Models 3–4 in Mae Moh and Duke forests suggests that “extra” memory is originating from variations in R_n (and this addition is not mediated by the inclusion of s). This extra memory is most evident at the Duke Forest site, where seasonality in R_n is most pronounced.

It can be surmised that soil moisture spectra at longer time scales cannot be explained by only precipitation controls at all sites as assumed in DM88, and seasonality in radiative controls play a nontrivial role at such time scales. These radiative controls, needed when assessing the role of regional dimming on the hydrological cycle, were included here using the Priestley-Taylor equation. The inclusion of a radiatively forced potential ET model above and beyond rainfall variability appears to improve predictions of soil moisture spectra at long time scales. The measured soil moisture memory (model decay time scale) for all three forests was about 25–38 days, which was larger than the evaporative damping time scale, except that these two time scales in the Seto forest were nearly the same. At the storm time scales, power law scaling in precipitation spectra (i.e., $E_p \sim f^{-\alpha}$) due to temporally autocorrelated storm activities leads to soil moisture spectra that scale as $f^{-2-\alpha}$. Net radiation variability, on the other hand, had no appreciable impact on such short time scales. Hence, a broad implication of these two findings is that the rapid decay in soil moisture spectra with increasing f provides justification to the use of daily stochastic rainfall in conventional ecohydrological models.

Acknowledgments

Katul acknowledges the National Science Foundation (NSF-AGS-1102227, NSF-CBET-103347, and NSF-EAR-1344703), the United States Department of Agriculture (2011-67003-30222), and the U.S. Department of Energy (DOE) through the Office of Biological and Environmental Research (BER) Terrestrial Carbon Processes (TCP) program (DE-SC0006967 and DE-SC0011461). We also thank the Japan Society for the Promotion of Science (JSPS) KAKENHI grants 24405031 and 20248016 for supporting the experiments at the Mae Moh and Seto forests, respectively. The data of Mae Moh and Duke forests for this study are available upon request to Igarashi (igarashi@hyarc.nagoya-u.ac.jp, Mae Moh forest) and Katul (gaby@duke.edu, Duke forest), respectively. The data of Seto forest is opened in the AsiaFlux database. More information about the data of Seto site can be found at http://asiaflux.net/index.php?page_id=104. This work was conducted under the framework of the “Precise Impact Assessments on Climate Change” of the Program for Risk Information on Climate Change (SOUSEI Program) supported by the Ministry of Education, Culture, Sports, Science, and Technology (MEXT) of Japan.

M. Bayani Cardenas thanks two anonymous reviewers for their assistance in evaluating this paper.

References

- Daly, E., A. C. Oishi, A. Porporato, and G. G. Katul (2008), A stochastic model for daily subsurface CO_2 concentration and related soil respiration, *Adv. Water Resour.*, *31*(7), 987–994.
- Delworth, T., and S. Manabe (1988), The influence of potential evaporation on the variabilities of simulated soil wetness and climate, *J. Clim.*, *1*, 523–547.
- Dirmeyer, P. A., Y. Jin, B. Singh, and X. Yan (2013), Trends in land-atmosphere interactions from CMIP5 simulations, *J. Hydrometeorol.*, *14*, 829–849.
- Fraedrich, K., and C. Larnder (1993), Scaling regimes of composite rainfall time series, *Tellus, Ser. A*, *45*(4), 289–293.
- Guan, K., S. E. Thompson, C. J. Harman, N. B. Basu, P. S. C. Rao, M. Sivapalan, A. I. Packman, and P. K. Kalita (2011), Spatiotemporal scaling of hydrological and agrochemical export dynamics in a tile-drained Midwestern watershed, *Water Resour. Res.*, *47*, W00J02, doi:10.1029/2010WR009997.
- Katul, G. G., A. Porporato, E. Daly, A. C. Oishi, H.-S. Kim, P. C. Stoy, J.-Y. Juang, and M. B. Siqueira (2007), On the spectrum of soil moisture from hourly to interannual scales, *Water Resour. Res.*, *43*, W05428, doi:10.1029/2006WR005356.
- Koster, R. D., and M. J. Suarez (2001), Soil moisture memory in climate models, *J. Hydrometeorol.*, *2*, 558–570.
- Kumagai, T., and A. Porporato (2012), Drought-induced mortality of a Bornean tropical rain forest amplified by climate change, *J. Geophys. Res.*, *117*, G02032, doi:10.1029/2011JG001835.
- Kumagai, T., G. G. Katul, T. M. Saitoh, Y. Sato, O. J. Manfroi, T. Morooka, T. Ichie, K. Kuraji, M. Suzuki, and A. Porporato (2004), Water cycling in a Bornean tropical rain forest under current and projected precipitation scenarios, *Water Resour. Res.*, *40*, W01104, doi:10.1029/2003WR002226.
- Lauzon, N., F. Anctil, and J. Petrinovic (2004), Characterization of soil moisture conditions at temporal scales from a few days to annual, *Hydrol. Processes*, *18*(17), 3235–3254.
- Li, H., A. Robock, and M. Wild (2007), Evaluation of Intergovernmental Panel on Climate Change fourth assessment soil moisture simulations for the second half of the twentieth century, *J. Geophys. Res.*, *112*, D06106, doi:10.1029/2006JD007455.
- Matsumoto, K., et al. (2008), Energy consumption and evapotranspiration at several boreal and temperate forests in the Far East, *Agric. For. Meteorol.*, *148*(12), 1978–1989.
- Miller, G. R., D. D. Baldocchi, B. E. Law, and T. Meyers (2007), An analysis of soil moisture dynamics using multi-year data from a network of micrometeorological observation sites, *Adv. Water Resour.*, *30*(5), 1065–1081.
- Milly, P. C. D., R. T. Wetherald, K. A. Dunne, and T. L. Delworth (2002), Increasing risk of great floods in a changing climate, *Nature*, *415*, 514–517.
- Molini, A., G. G. Katul, and A. Porporato (2009), Revisiting rainfall clustering and intermittency across different climatic regimes, *Water Resour. Res.*, *45*, W11403, doi:10.1029/2008WR007352.
- Montosi, E., S. Manzoni, A. Porporato, and A. Montanari (2012), An ecohydrological model of malaria outbreaks, *Hydrol. Earth Syst. Sci.*, *16*, 2759–2769.
- Moore, G. W., J. A. Jones, and B. J. Bond (2011), How soil moisture mediates the influence of transpiration on streamflow at hourly to interannual scales in a forested catchment, *Hydrol. Processes*, *25*(24), 3701–3710.
- Parent, A. C., A. Francois, and L.-E. Parent (2006), Characterization of temporal variability in near-surface soil moisture at scales from 1 h to 2 weeks, *J. Hydrol.*, *325*, 56–66.
- Parlange, M. B., G. G. Katul, R. H. Cuenca, M. L. Kavvas, D. R. Nielsen, and M. Mata (1992), Physical basis for a time series model of soil water content, *Water Resour. Res.*, *28*, 2437–2446, doi:10.1029/92WR01241.

- Porporato, A., E. Daly, and I. Rodriguez-Iturbe (2004), Soil water balance and ecosystem response to climate change, *Am. Nat.*, *164*(5), 625–632.
- Potts, D. L., R. L. Scott, S. Bayram, and J. Carbonara (2010), Woody plants modulate the temporal dynamics of soil moisture in a semi-arid mesquite savanna, *Ecohydrology*, *3*(1), 20–27.
- Priestley, C. H. B., and R. J. Taylor (1972), On the assessment of surface heat flux and evaporation using large-scale parameters, *Mon. Weather Rev.*, *100*, 81–92.
- Priestley, M. B. (1981), *Spectral Analysis and Time Series*, 877 pp., Elsevier, New York.
- Seneviratne, S. I., et al. (2006), Soil moisture memory in AGCM simulations: Analysis of global land-atmosphere coupling experiment (GLACE) data, *J. Hydrometeorol.*, *7*, 1090–1112.
- Thompson, S. E., and G. G. Katul (2012), Multiple mechanisms generate Lorentzian and $1/f^a$ power spectra in daily stream-flow time series, *Adv. Water Resour.*, *37*, 94–103.
- Vinnikov, K. Y., A. Robock, N. A. Speranskaya, and C. A. Schlosser (1996), Scales of temporal and spatial variability of midlatitude soil moisture, *J. Geophys. Res.*, *101*(D3), 7163–7174.
- Welch, P. D. (1967), The use of fast Fourier transform for the estimation of power spectra: A method based on time averaging over short, modified periodograms, *IEEE Trans. Audio Electroacoust.*, *15*(2), 70–73.
- Wu, C., et al. (2012), An underestimated role of precipitation frequency in regulating summer soil moisture, *Environ. Res. Lett.*, *7*(2), 024011, doi:10.1088/1748-9326/7/2/024011.
- Wu, W., M. A. Geller, and R. E. Dickinson (2002), The response of soil moisture to long-term variability of precipitation, *J. Hydrometeorol.*, *3*, 604–613.
- Yoshifuji, N., T. Kumagai, K. Tanaka, N. Tanaka, H. Komatsu, M. Suzuki, and C. Tantasirin (2006), Inter-annual variation in growing season length of a tropical seasonal forest in northern Thailand, *For. Ecol. Manage.*, *229*, 333–339.
- Yoshifuji, N., Y. Igarashi, N. Tanaka, K. Tanaka, T. Sato, C. Tantasirin, and M. Suzuki (2014), Inter-annual variation in the response of leaf-out onset to soil moisture increase in a teak plantation in northern Thailand, *Int. J. Biometeorol.*, *58*, 2025–2029, doi:10.1007/s00484-013-0784-2.